Formation and Physicochemical Characterization of Silica-Based Blackberry-like Nanoparticles Capped by Polysaccharides

ARTICLE *in* THE JOURNAL OF PHYSICAL CHEMISTRY C · NOVEMBER 2007

Impact Factor: 4.77 · DOI: 10.1021/jp073037f

4 AUTHORS:

Patrizia Andreozzi
IFOM-FIRC Institute of Molecular Oncology
20 PUBLICATIONS **317** CITATIONS
SEE PROFILE

Camillo La Mesa
Sapienza University of Rome
133 PUBLICATIONS **1,830** CITATIONS
SEE PROFILE

Giancarlo Masci
Sapienza University of Rome
48 PUBLICATIONS **1,081** CITATIONS
SEE PROFILE

Lorenza Suber
Italian National Research Council
67 PUBLICATIONS **1,237** CITATIONS
SEE PROFILE

Formation and Physicochemical Characterization of Silica-Based Blackberry-like Nanoparticles Capped by Polysaccharides

Patrizia Andreozzi,[†,‡] Camillo La Mesa,*[,†,‡] Giancarlo Masci,[†] and Lorenza Suber[§]

Dipartimento di Chimica and SOFT-INFM-CNR Research Center, Università "La Sapienza", Piazzale A. Moro 5, Rome I-00185, Italy, and ISM-CNR, Via Salaria, Km 29.300, Monterotondo Stazione, (RM), Rome I-00016, Italy

Received: April 19, 2007; In Final Form: June 29, 2007

Strictly monodisperse 200-nm silica nanoparticles were hydrophobically modified (HM) by surface coverage with octadecanol. In successive stages, a graft copolymer was adsorbed. The graft copolymer was obtained by atom-transfer radical polymerization (ATRP). The polymer hydrophobic functionality consists of short pMMA [poly(methyl methacrylate)] units of controlled length and low polydispersity covalently linked to pullulan. Depending on concentration, it forms more or less densely packed layers on the surface of HM silica nanoparticles. The surface coverage density of these particles is modulated by the mole ratios between the components (grafted copolymer and HM nanoparticles) and is controlled by the solvent properties. The conditions used in surface coverage procedures, obtained by mixing the components in DMF and adding water in continuous elution gradient, give rise to uniformly polymer-grafted nanoparticles and to blackberry-like particles under saturation conditions. In such systems, the polar groups in the polymer chains face outward from the particles and give rise to corrugations on their surface. The surface morphology of the nanoparticles is tuned by controlling the amount of adsorbed polymer. In each stage of the surface coverage procedures, the resulting nanoparticles were investigated by DLS (in back-scattering mode) and SEM. The same holds for electrophoretic mobility results, which are rationalized in terms of a Langmuir-like adsorption isotherm.

Introduction

Nanoparticle technologies are of outstanding relevance in a wide variety of applications, spanning from the formation of colloid crystals and glasses[1,2] to paints and coatings[3] and from analytical separation[4] to biomedical- or bioremediation-oriented technologies.[5−7] Particularly attractive are technologies related to nanoparticle coverage by heparin,[8] polyelectrolytes, polysaccharides,[9] proteins,[10,11] and DNA.[12] These procedures lead to surface functionalization,[13,14] and the resulting objects serve, for instance, in biomimetic chemistry.[15]

Current technologies offer the opportunity to prepare particles for ad hoc applications through layer-by-layer adsorption of selected species and chemical functionalities.[16] As a result, simple protocols allow for the transformation of hydrophilic surfaces into hydrophobic ones; more exotic functionalization procedures are also possible.[17] As a result of the above transformations, flat surfaces can be transformed into highly porous ones, for instance. In some cases, the nanoparticle surfaces are engineered in such a way as to allow the selective adsorption of components from biological fluids in contact with the particles. Some components of these fluids interact selectively with the functionalized entities; others are released.

In this contribution, modifications of hydrophobically modified (HM) silica coated by polar graft copolymers through iterative coverage procedures are addressed, and some results relative to a selected system are reported. Graft copolymers obtained by grafting poly(methyl methacrylate) (pMMA) chains onto pullulan by atom-transfer radical polymerization (ATRP) were used.[18] Pullulan was chosen because of its flexibility compared to other polysaccharides, such as cellulose or chitosan.[19] Grafted pullulan might allow densely covered surfaces to be obtained by adsorption onto HM silica nanoparticles, provided that their hydrophobic modification degree is moderate and that there is room for graft adsorption on such nanoparticles.

The resulting materials were investigated by combining information from dynamic light scattering (DLS), scanning electron microscopy (SEM), and electrophoretic mobility. DLS and SEM provide information on particle size and morphology, respectively; electrophoretic measurements provide information on the extent of surface coverage. Electrophoretic mobility can determine how much the adsorbed polymer modifies the electrical double layer around functionalized nanoparticles and the resulting stability to sedimentation, or creaming. In such cases, the amount of electrolyte in the medium must be lower than the critical flocculation threshold.

Effort is made to relate electrophoretic mobility results to polymer adsorption onto nanoparticles. Such values are rationalized on proper grounds by using a Langmuir-like adsorption isotherm. The subsequent elaboration offers the opportunity to relate the residual particle charge density to surface coverage.

Experimental Section

Materials. H_2O was doubly distilled in a Pyrex all-glass apparatus over alkaline $KMnO_4$. The ionic conductivity of freshly distilled water, χ, is between 0.7 and 1.0 μS cm^{-1} at 25.00 °C. NH_3, 33.0 vol % (Carlo Erba) was used. DMF (Aldrich) was dehydrated by refluxing over thermally activated

* Corresponding author. Tel.: +39-06-491694 (direct) or +39-06-49913707. Fax. +39-06-490631. E-mail: camillo.lamesa@uniroma1.it.
† Dipartimento di Chimica, Università "La Sapienza".
‡ SOFT-INFM-CNR Research Center, Università "La Sapienza".
§ ISM-CNR.

10.1021/jp073037f CCC: $37.00
Published on Web 11/16/2007 PAGE EST: 5.9

SCHEME 1: Representation of $PU_{5,3}$-*g*-$pMMA_{22}$, Denoted PU-graft[a]

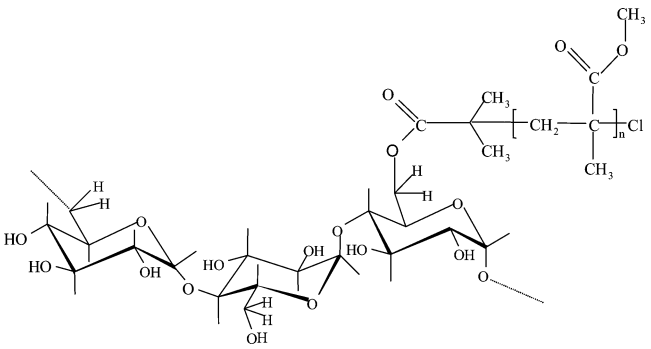

[a] 5.3 is the number of grafts per 100 sugar units, and 22 is the number-average degree of polymerization (X_n) of the pMMA chains.

$MgSO_4$ and distilled at 80 °C and 60 mmHg. Octadecanol (C_{18}, Sigma Aldrich) was used as received.

Tetraethyl orthosilicate (TEOS, Sigma-Aldrich) and absolute ethanol (Sigma-Aldrich) were vacuum distilled. Other solvents (Sigma Aldrich) were of analytical purity.

Pullulan (PU, PF-20, Hayascibara Co. Ltd., Okayama, Japan) is a linear natural extracellular polysaccharide, from *Aureobasidium pullulans*, consisting of (1−6)-α-D-linked maltotriosyl units. Its viscosity-average molecular mass, M_v, is 1.7×10^5 Da. Its chain is mobile and elastic compared to most naturally occurring polysaccharides. On these grounds, it is expected that PU derivatives can adsorb extensively onto surfaces and ensure them a significant coverage, because of the reasons given above. In Scheme 1 is schematically drawn a picture of a grafted pMMA-based pullulan derivative.

Sodium azide (Sigma Aldrich) was added in small amounts (3−5 mmol kg^{-1}) to aqueous dispersions of the polymer-coated nanoparticles, in order to modulate their ionic strength and eventually minimize microbial attacks to grafted pullulan. At the same time, the salt concentration must be lower than the value required for critical flocculation conditions.

Material Preparation. *Silica.* Silica was prepared by hydrolysis of TEOS in ethanol, according to standard procedures.[20] To this end, 150 mL of absolute ethanol, 8.0 mL of H_2O, and 4.27 mL of freshly distilled TEOS were added to 4.5 mL of ammonia (30%). Twenty minutes after the addition of NH_3, an increase in turbidity was observed, and the solution became slightly opalescent. Two hours later, 1.0 mL TEOS was added, and hydrolysis proceeded for 30 h at room temperature under mild stirring. Particle size was found to be proportional to the amounts of water and NH_3 in the medium; nanospheres (diameter close to 200 nm) were obtained by choosing proper mole ratios between the components.[21,22]

The final silica dispersions were refluxed under nitrogen flow, to eliminate NH_3. To avoid collapse, the particles were kept in ethyl ether until use. When required, they were recovered by dialysis and dispersed in the required solvent. The size polydispersity index, Pd_i (the second moment inferred by DLS), was lower than 5%.

Hydrophobic Modification. Stabilization was performed by adsorbing octadecanol,[21,23] to avoid coagulation and subsequent formation of silica particles clusters. The alkanol also allowed significant hydrophobic interactions with the graft copolymer. Solid octadecanol (C_{18}, 4.1 g) was added to 1.0 g of freshly prepared silica dissolved in 5.0 mL of ethanol. Surface functionalization proceeded under stirring and N_2 flow at 170 °C for 3 h. Excess C_{18} and impurities were removed by washing 3 times and centrifuging in absolute ethanol. The resulting HM particles were dried at 60 °C under N_2 flow, washed in proper solvents, and dispersed in ethyl ether or DMF until use.

The procedures used for hydrophobic functionalization by C_{18} required care, to minimize loss of particles. The high temperatures required to allow the reaction of SiO_2 with C_{18} also helped eliminate ethanol and water from the reaction medium. At room temperature, the resulting product was a dispersion of modified particles in a high-melting-point waxy solid, and care had to be taken to avoid unwanted losses by rapid cooling of the dispersions. Ethanol was used to purify the HM nanoparticles. Successive washing with DMF minimized the amount of free octadecanol. DMF was chosen because it is an excellent solvent for the long-chain alcohol and a good dispersant for C_{18}-covered nanoparticles and PU-graft as well.

The nanoparticle mass was converted into volume fraction, Φ. The mass of HM silica was determined by drying suspensions of the particles in a vacuum and assuming that only the low-boiling species were removed. Given the masses of the dispersion (m_s) and the dry particles (m_p) and the densities of the solvent ($\rho_s = 0.94$ g cm^{-3}) and silica ($\rho_p = 2.10$ g cm^{-3}) and neglecting the contribution due to the grafted long-chain alkanol, the volume fraction was obtained as

$$\Phi = \left[\frac{\left(\frac{m_p}{\rho_p}\right)}{\left(\frac{m_p}{\rho_p}\right) + \left(\frac{m_s}{\rho_s}\right)} \right] \quad (1)$$

The values of the volume fraction were in the range of $(3-7) \times 10^{-3}$.

HM Pullulan. PU was grafted with pMMA according to a "grafting from" method by atom-transfer radical polymerization (ATRP), as already described in a previous work.[18] Briefly, a pullulan macroinitiator (PU−B*i*B) was prepared by reacting pullulan with α-bromoisobutyryl bromide (B*i*BBr), giving a derivative with a degree of substitution (DS, the number of B*i*B groups introduced per 100 glucose units of pullulan) of 5.3% (PU−B*i*$B_{5.3}$). The pullulan macroinitiator was used to initiate the ATRP of MMA using an initial MMA concentration of 1.5 M, and initial concentration ratios of MMA/Pull-B*i*$B_{5.3}$/CuCl/$CuCl_2$/bpy = 50:1:1:0.6:4 and water/DMF 20:80 (v/v) at 50 °C. The polymerization was stopped at about 44% conversion, to obtain a number-average degree of polymerization (X_n) of the pMMA chains of about 22. The resulting product is denoted $PU_{5,3}$-*g*-pMMA22, or PU-graft.[18]

Particle Functionalization by the Graft Copolymer. $PU_{5,3}$-*g*-$pMMA_{22}$ was dissolved in DMF for the reasons given above. An appropriate amount of the polymer solution (in slight excess with respect to that required for complete adsorption) was mixed into a DMF mixture containing the HM nanoparticles. The resulting dispersion was injected with water to reach a volume fraction ratio with respect to DMF of close to 3:1. Water injection was made at a speed of 0.49 mL h^{-1}, under mild stirring, at room temperature. Mixing in continuous elution gradient avoided foaming and reduced particle losses. The final dispersion in the mixed solvent was extensively dialyzed against water, until the refractive index of the medium matched that of distilled H_2O. The cutoff size of the cellulose membranes was 12 kD.

Methods. *SEM Microscopy.* Measurements were performed at 20 kV with a SEM-LEO1450VP instrument, equipped with an INCA300 EDS microanalysis unit.[24,25] Drops of aqueous (or DMF) dispersions were stratified onto accurately polished

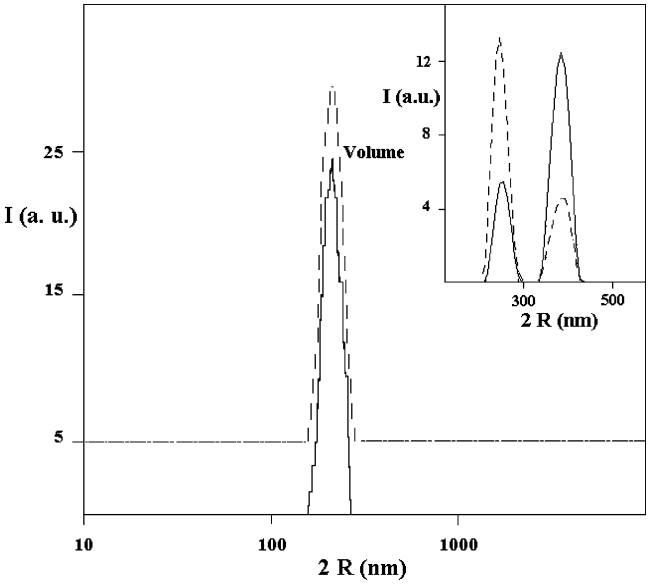

Figure 1. Comparison between volume (dotted line) and intensity statistics (full line) as obtained by DLS in back-scattering mode for 5.9×10^{-3} Φ (in volume fraction) HM silica in DMF at 25.0 °C. Data are reported as number of counts (*I*, au) vs size (2*R*) on a semilogarithmic scale. In the inset, the volume and intensity statistics are compared for the case of association. Data therein refer to 4.9×10^{-3} Φ silica in a poor solvent, such as ethanol, at 25.0 °C.

optical microscopy glass slides (2.0 × 2.0 cm), and the liquids were removed by gentle heating. To minimize mass loss and enhance medium conductivity (the particles are poor conductors), HM and copolymer-coated nanoparticles were covered in gold by vapor sputtering. SEM images were collected and elaborated according to standard procedures.

DLS Analysis. A Malvern Nano ZS series HT instrument was used to perform DLS measurements in back-scattering mode at 632.8 nm and 173°, at 25.0 ± 0.1 °C.[26] The apparatus performances were controlled by measuring the size of 100-nm monodisperse polystyrene latex spheres in water, stabilized by tiny amounts of anionic charges from sulfate groups (Alfa Aesar). The data analysis facility elaborated the decay-time distribution functions using a CONTIN algorithm.

Particle sizes determined by DLS were constant to within a few percent. Data are reported in terms of intensity and volume statistics,[27] to ascertain whether true monodispersity held (Figure 1). The DLS results indicated that the particles were monodisperse in size and the clustering was moderate (except in the case of poor solvents, such as ethanol for raw silica; see the inset of Figure 1).

ζ *Potential.* A Malvern laser-velocimetry Doppler instrument (HT ZS Nano series) was used to determine the electrophoretic mobility, μ, by taking the average of several individual scans. The solutions were located in U-shaped cuvettes equipped with gold-coated electrodes.[28] The temperature was set to 25.0 ± 0.1 °C by a Peltier unit. The apparatus performances were checked by determining the electrophoretic mobility of sulfonated 100-nm polystyrene latex spheres (Aldrich). Aqueous solutions used as particles dispersants were added with 3.0 mmol kg^{-1} NaN_3 as a supporting electrolyte. The above concentration was well below the critical flocculation value of HM silica (about 20 mmol kg^{-1}) and ensured a significant stability to the dispersions.

Experimental μ values were obtained by scanning the applied potential from −150 to 150 mV. μ values were taken at the maximum of the intensity distribution function (number of counts) vs *V* (Figure 2). Data were transformed into ζ potential values according to[29]

$$\zeta = \left(\frac{4\pi\eta\mu}{\epsilon}\right) \qquad (2)$$

where ζ is the ζ potential (measured at the maximum of the function), ϵ is the dielectric constant of the dispersing medium, and η is the solvent viscosity. Errors on ζ values were a few percent.

At low ionic strength, Hückel's approximation holds, and Henry's law is fulfilled.[30] The mobility is corrected multiplying eq 2 by $f(\kappa a)$, where $1/\kappa$ is the Debye length, related to the electrical double-layer thickness, and *a* is the particle radius. Accordingly

$$\zeta f(\kappa a) = \left(\frac{4\pi\eta\mu}{\epsilon}\right) \rightarrow \zeta = \left(\frac{6\pi\eta\mu}{\epsilon}\right) \qquad (2')$$

In all cases, Hückel's approximation holds when $f(\kappa a)$ approaches $^2/_3$.[31]

Refractive Index. An Abbe refractometer (Galileo) operating in the range of 1.3−1.7 was used. The unit was thermostatted at 25.0 ± 0.05 °C by an external circulation bath (Heto). The resolution on *n* values was better than 1×10^{-4} units.

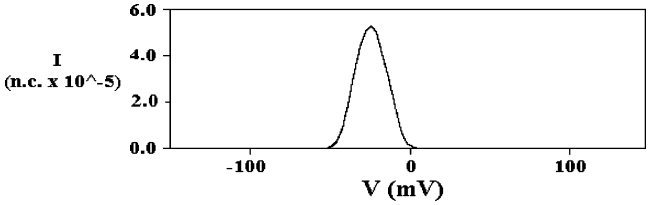

Figure 2. ζ potential plot, reported as intensity (*I*, number of counts × 10^{-5}) versus applied voltage (*V* in mV), for an aqueous dispersion containing 6.1×10^{-3} Φ HM silica particles in 3.0 mm NaN_3 at 25.0 °C.

SCHEME 2: Nanoparticle Preparation and Purification Procedures

Reagent(s)	*Conditions*	*Purification*	*Product*	*Characterisation*
TEOS	*(ethanol)*		*SiO_2*	*DLS, SEM*
	NH_3-H_2O, r.t.	*(ethanol)*		
SiO_2 + C_{18}	*(ethanol)*		*C_{18} SiO_2*	*DLS, SEM*
	170° C	*(ethanol)*		
		(DMF)		
C_{18} SiO_2 +PU-graft	*(DMF added*		*PU-graft|$C_{18}SiO_2$*	*DLS, SEM*
	with H_2O), r.t.	*(H_2O)*		

TABLE 1: Size of Octadecanol-Covered HM Silica Nanoparticles (in nm) in Different Solvent Media, as Inferred by DLS and SEM[a]

solvent	DLS, *z* average	SEM
H_2O	220 ± 0	210 ± 10
DMF	250 ± 15	230 ± 10
THF	220 ± 10	220 ± 10
CY	230 ± 15	220 ± 15

[a] Light scattering data refer to volume fractions in the range of 5−6 × 10^{-3}; SEM values were obtained after the dispersions had been dried.

Results and Discussion

Particle Preparation. Before describing the characterization of the particles, we report a step-by-step scheme of their

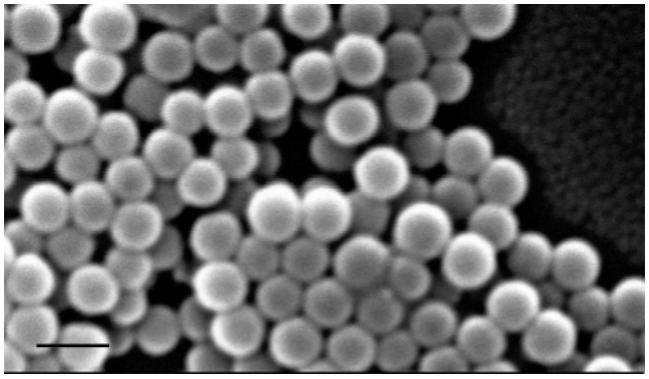

Figure 3. SEM image of HM silica nanoparticles, formerly dispersed in ethyl ether, adsorbed onto glass. The size of the bar at the bottom of the figure is 300 nm.

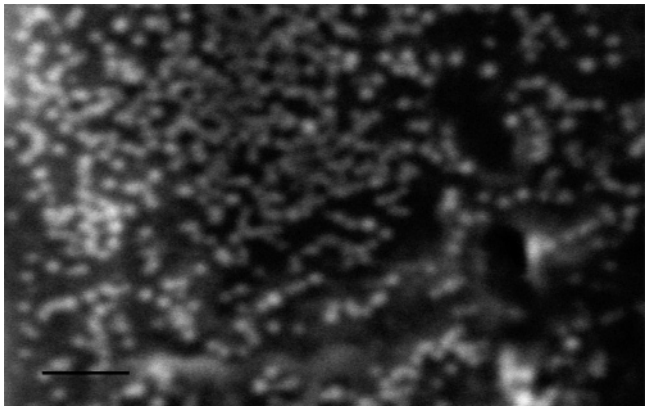

Figure 4. SEM image of PU-graft-based macromolecules, obtained by drying the corresponding DMF solutions onto glass. The bar size at the bottom of the figure is 300 nm.

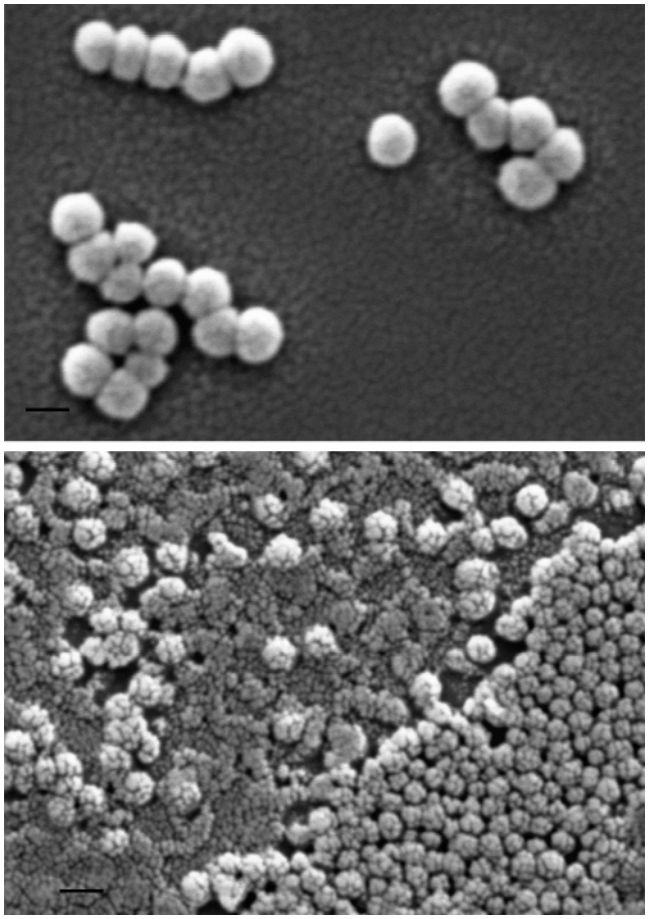

Figure 5. SEM images of (a) HM silica nanoparticles, functionalized with tiny amounts of PU-graft, and (b) the same particles saturated by the above polymer, which is clearly seen on the sample holder. The size of the bars at the bottom of both figures is 300 nm.

preparation. Scheme 2 indicates the procedures required to obtain the products in high yields and the related purification steps.

Particle Characterization. Ethanolic solutions of silica nanoparticles, obtained according to the method of Stober et al.,[20] were characterized by DLS and SEM. The results indicate a progressive collapse of the particles in the given medium and the appearance of a bimodal size distribution function with time (inset in Figure 1). Particles stabilized by octadecanol, conversely, are monodisperse in size. They coagulate in water, to minimize contact with that solvent; indeed, transfer from H_2O to organic solvents gives strictly monodisperse entities. The particle size distribution function obtained by DLS was centered around 220 nm and was nearly insensitive to the dispersing medium, either DMF, THF, DMSO, or cyclohexane. Minor effects arose from a partial swelling of the octadecanol adsorbed layer (Table 1).

Electron Microscopy. SEM images, obtained by placing drops of the above solutions onto glass and drying (with eventual gold coverage), indicate that raw and HM nanoparticles are highly monodisperse in size and that their surface is flat. No holes or pores could be observed even at high magnifications (Figure 3).[32] In SEM images of particles covered with PU-graft, some polymer-based (presumably unimolecular) 40-nm polymeric units can be observed as dots (Figure 4). Their contribution to the total scattering intensity in water is negligible, as they are almost traceless in DLS plots.

Polymer Adsorption. $PU_{5.3}$-*g*-$pMMA_{22}$ is an amphiphilic grafted derivative soluble in DMF, a good solvent for both pullulan and pMMA, whereas in water, it forms nanoparticles with a pMMA core and a pullulan shell.[33] $PU_{5,3}$-*g*-$pMMA_{22}$ solubilized in DMF progressively binds onto HM silica upon addition of water, preferring adsorption to micelle formation.

DLS indicates that PU-graft behaves as a whole kinetic entity with the nanoparticles and that almost no free polymer is detected. It is reasonable to assume that PU-graft quantitatively forms polymer layer(s) on the nanoparticles. To confirm the above hypothesis, a solution containing nanoparticles, at $\Phi = 5.93 \times 10^{-3}$, were added to equal volumes of the same solvent containing 0.37 mg mL^{-1} PU-graft. The resulting mixture was added to excess water, according to the procedures reported above. The dispersing medium becomes a poor solvent for particles and grafted polymer, which self-assemble to minimize hydrophobic interactions with water. Phase separation is induced, but no free polymer can be detected in the medium.

Under such conditions, significant surface coverage occurs, as indicated by SEM (Figure 5). There is no difference, in this regard, from HM silica coverage by surfactant molecules.[34,35] Similar results were obtained by adding lower amounts of $PU_{5,3}$-*g*-$pMMA_{22}$ to HM silica nanoparticles. (Note that the concentrations of the individual batches are given in Table 2.) In all cases, the graft polymer adsorbs quantitatively onto HM silica. The final dispersions in 3.0 mmol kg^{-1} water$-NaN_3$ as the solvent are stable and flocculation, if any, is slow.

According to SEM, surface coverage is proportional to the amount of added $PU_{5,3}$-*g*-$pMMA_{22}$ in the mixture (Figure 5a,b). The presence of excess polymer coexisting with surface-saturated particles can be observed, conversely, in Figure 5b.

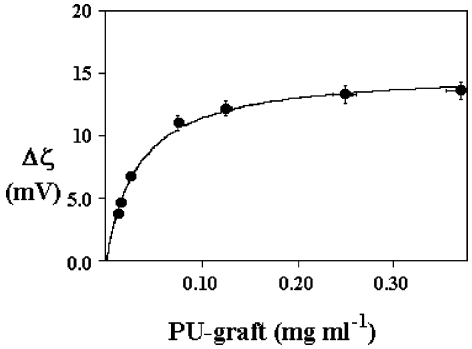

Figure 6. ζ potential (mV) vs the amount of added PU-graft in the reaction medium (mg mL^{-1}) at 25.0 °C. ζ potential values were rescaled with respect to the original value.

TABLE 2: Amount of $Pull_{5,3}$-*g*-$pMMA_{22}$ Used to Cover the Particles

$Pull_{5,3}$-*g*-$pMMA_{22}$ (mg/mL)	volume of DMF (mL)
0.013	1.898
0.015	1.882
0.022	1.827
0.026	1.795
0.075	1.408
0.125	1.014
0.250	0.028
0.375	0.000

Light scattering experiments on the above dispersions indicate that the correlation function is strictly monoexponential (with the exception of raw silica in ethanol), the size distribution function is narrow, and the polydispersity index is low. The constancy of the particle hydrodynamic radius, R_H, throughout the whole range of $PU_{5,3}$-*g*-$pMMA_{22}$-to-HM silica ratios indicates that surface coverage is uniform. This hypothesis was confirmed by electrophoretic mobility and is discussed below.

Electrophoretic Mobility. Raw electrophoretic mobility measurements as a function of the nominal PU-graft content in the medium, reported in Figure 6, indicate the occurrence of surface saturation. The relations between the ζ potential and the surface charge density of these particles, σ, imply that

$$\sigma = \left(\frac{\epsilon\zeta}{4\pi\tau}\right) = \left(\frac{\eta\mu}{\tau\bar{E}}\right) \tag{3}$$

where τ is the double-layer thickness and $\bar{E}$ is the applied electric field.

In terms of the double-layer theory, τ depends on the medium ionic strength,[36] which is kept nearly constant by added NaN_3, and modifications in σ values are mostly due to particle coverage. Accordingly

$$\sigma = \left[1 - \left(\frac{Z\theta_s}{N}\right)\right]\left(\frac{e}{f_0}\right) \tag{4}$$

where θ_s is the fractional surface coverage by PU-graft, *Ze* is the charge of adsorbed ions at the given pH and ionic strength, and *N* is the number of polymer subunits of area f_0 each. The ratio e/f_0, the area covered by a charge entity, can be expressed as a surface charge density per unit area, σ_0.[37,38] When $Z = 1$, as in the present case, eq 4 can be rearranged as

$$N\left[1 - \left(\frac{\sigma}{\sigma_0}\right)\right] = N\sigma_{red} = \theta_s \tag{4'}$$

In other words, σ_{red} and θ_s are strictly interrelated.

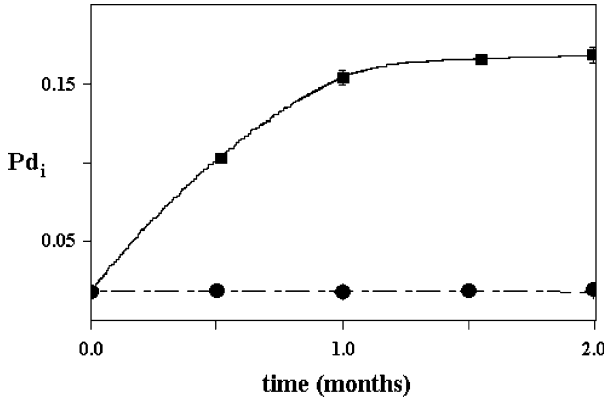

Figure 7. Polydispersity index (PDI) vs time (in months) for PU-graft-covered nanoparticles (circles) and HM silica nanoparticles (squares) as inferred from DLS intensity statistics plots at 25.0 °C. Size was obtained from the correlation function using the CUMULANT algorithm fitting a single exponential to the correlation function to obtain the mean size (*z*-average diameter) and an estimate of the width of the distribution (polydispersity index).

Equation 4′ can quantify surface coverage by combination with a classical form of the Langmuir adsorption isotherm. For systems at equilibrium in the presence of a finite bulk concentration, the ratio between adsorbed polymer and complete coverage conditions conforms to

$$\theta_s = \left(\frac{q_{ads}}{q_{sat}}\right) = \left(\frac{bq_{bulk}}{1 + bq_{bulk}}\right) \tag{5}$$

where q_{ads}, q_{sat}, and q_{bulk} are the amount of adsorbed PU-graft at a given concentration, the surface saturation threshold, and the amount of nonadsorbed polymer, respectively. *b* is a proper constant. Polymer binding is an irreversible adsorption process in water, and the saturation concentration was assumed to be equal to the equilibrium conditions in the original solvent medium. In fact, almost no free polymer was present in the aqueous dispersions. In addition, no $PU_{5,3}$-*g*-$pMMA_{22}$ micelles were observed (see above). The residual amount of free PU-graft in the reacting medium (DMF + H_2O) was evaluated by refractive index measurements. In this way, estimates on the extent of surface coverage can be made.

A perusal of Figure 6 indicates that surface coverage qualitatively fulfills Langmuir-like behavior, with saturation at high PU-graft-to-HM nanoparticle ratios. The covered particles are stable in H_2O-NaN_3 and do not release PU-graft. This is evidenced by plotting the time evolution of the polydispersity index, Pd_i, vs time, as in Figure 7. As can be inferred from this figure, PU-graft-covered nanoparticles reduce their size only slightly and, at the same time, retain polydispersity even after a prolonged stay in water. Conversely, such conditions are not fulfilled in octadecanol HM silica.

Changes in surface charge density are associated with polymer adsorption on the particles, and the adsorbed amount can be evaluated from the ζ potential. For consistency, data in Figure 6 were rescaled with respect to the initial value. This procedure, however, did not modify the fit quality. At high surface coverage, the particles were relatively stable, even though the ζ potential values were low. This behavior presumably arises from the significant interactions of the hydrophilic portion of PU-graft with water.

Some more questions can be considered. In principle, the hypothesis of incomplete surface coverage by octadecanol cannot be ruled out. Surface charge density results relative to silica covered by octanol, in particular, indicate that surface

coverage might not be complete. The surface charge density, σ, is 3.9 mC cm^{-2} for raw silica and 3.1 mC cm^{-2} for the octanol HM sample.[39] The variation due to hydrophobic modification in the present system is more significant, and the final octadecanol HM particles have σ values close to 1.6 mC cm^{-2}. Even though the silica particles were only moderately covered, the functionalization process played by PU-graft would not be hindered, as the pMMA chains have enough room to settle on the surface and cover it. This hypothesis is consistent with previous work.[40] Thus, provided that a significant amount of the particle surface is functionalized, binding of HM polymers therein would be noticeable.

As far as aging is concerned, some shrinking was observed at long times. Similar conclusions were drawn by other authors[41−43] and ascribed to significant polymer compaction on the particle surface. Even though some shrinking of the polymer layer occurs, no links between polydispersity and size were observed, as indicated in Figure 7. It is thus reasonably assumed that the process does not imply detachment of PU-graft from the functionalized nanoparticles. Thus, $PU_{5,3}$-*g*-$pMMA_{22}$ molecules, firmly bound to the nanoparticles, can self-compact with time, in analogy with what was previously observed for the adsorption of lauroyl-based HM−PU at the air-aqueous solution interface.[44]

Conclusions

Silica nanoparticles were functionalized in successive stages by octadecanol and by subsequent absorption of $PU_{5,3}$-*g*-$pMMA_{22}$. The resulting nanoparticles showed flat or corrugated surfaces, depending on the amount of adsorbed graft copolymer. Close to saturation, the functionalized objects assumed a blackberry-like structure, with the polysaccharide units facing outward toward the bulk. The covered nanoparticles were stable and did not show a significant tendency toward flocculation.

Surface coverage by $PU_{5,3}$-*g*-$pMMA_{22}$ was quantified by SEM and ζ potential measurements. The results indicated that adsorption is concomitant with changes in electrophoretic mobility and that direct proportionality exists between surface coverage and ζ potential values. Binding onto such nanoparticles was rationalized in terms of a simplified Langmuir adsorption isotherm.

Further advances in the field are promising and could allow for further binding of macromolecules onto hydrophilic surfaces covered by polysaccharides. This can be achieved by chemical bonding to nanoparticles and/or specific adsorption therein. Polysaccharide-covered particles are of outstanding relevance in a wide number of possible applications.

For these purposes is required a deep characterization of their biocompatibility in real biological matrices and, in particular, their tolerance to pH or ionic strength shocks should be determined. Such aspects could be developed in future work.

References and Notes

(1) (a) Wang, J.; Li, Q.; Knoll, W.; Jonas, U. *J. Am. Chem. Soc.* **2006**, *128*, 15606. (b) Paquet, C.; Yoshino, F.; Levina, L.; Gourevich, I.; Sargent, E. H.; Kumacheva, E. *Adv. Funct. Mater.* **2006**, *16*, 1892.

(2) Russell, E. V.; Israeloff, N. E. *Nature* **2000**, *408*, 695.

(3) Holme, I. *Surf. Coatings Int. B: Coatings Trans.* **2006**, *89*, 343.

(4) Yoshimatsu, K.; Reimhult, K.; Krozer, A.; Mosbach, K.; Sode, K.; Ye, L. *Anal. Chim. Acta* **2007**, *584*, 112.

(5) Schwalbe, M.; Pachmann, K.; Hoeffken, K.; Clement, J. H. *J. Phys. Condens. Matter* **2006**, *18*, S2865.

(6) Magnani, M.; Galluzzi, L.; Bruce, I. J. *J. Nanosci. Nanotechnol.* **2006**, *6*, 2302.

(7) Minc, N.; Slovakova, M.; Dorfman, K. D.; Bokov, P.; Bilkova, Z.; Smadja, C.; Futterer, C.; Taverna, M.; Viovy, J.-L. In *Micro Total Analysis Systems 2004*; Laurell, T., Nilsson, J., Jensen, K., Harrison, D. J., Eds.; Royal Society of Chemistry: Cambridge, U.K., 2004; Vol. 1, Paper 296530.

(8) (a) Lamprecht, A.; Koenig, P.; Ubrich, N.; Maincent, P.; Neumann, D. *Nanotechnology* **2006**, *17*, 3673. (b) Guo, J.; Amemiya, S. *Anal. Chem.* **2006**, *78*, 6893.

(9) (a) Gu, M.-Q.; Yuan, X.-B.; Kang, C.-S.; Zhao, Y.-H.; Tian, N.-J.; Pu, P.-Y.; Sheng, J. *Carbohydr. Polym.* **2007**, *67*, 417. (b) Bertholon, I.; Ponchel, G.; Labarre, D.; Couvreur, P.; Vauthier, C. *J. Nanosci. Nanotechnol.* **2006**, *6*, 3102.

(10) Duchesne, L.; Fernig, D. G. *Anal. Biochem.* **2007**, *362*, 287.

(11) Li, D.; Teoh, W. Y.; Selomulya, C.; Woodward, R. C.; Amal, R.; Rosche, B. *Chem. Mater.* **2006**, *18*, 6403.

(12) (a) Rittich, B.; Spanova, A.; Horak, D.; Benes, M. J.; Klesnilova, L.; Petrova, K.; Rybnikar, A. *Colloids Surf. B: Biointerfaces* **2006**, *52*, 143. (b) Bauer, M.; Haglmueller, J.; Pittner, F.; Schalkhammer, T. *J. Nanosci. Nanotechnol.* **2006**, *6*, 3671.

(13) Dujardin, E.; Mann, S. *Adv. Mater.* **2002**, *14*, 775.

(14) Kinsella, J. M.; Ivanisevic, A. *Langmuir* **2007**, *23*, 3886.

(15) Klem, M. T.; Young, M.; Douglas, T. *Mater. Today* **2005**, *8*, 28.

(16) Caruso, F. *Adv. Mater.* **2001**, *13*, 11.

(17) Kulak, A.; Davis, S. A.; Dujardin, E.; Mann, S. *Chem. Mater.* **2003**, *15*, 528.

(18) Bontempo, D.; Masci, G.; De Leonardis, P.; Mannina, L.; Capitani, D.; Crescenzi, V. *Biomacromolecules* **2006**, *7*, 2154.

(19) (a) Tahlawy, K. E.; Hudson, S. M. *J. Appl. Polym. Sci.* **2003**, *89*, 901. (b) Durand, A.; Marie, E.; Rotureau, E.; Leonard, M.; Dellacherie, E. *Langmuir* **2004**, *20*, 6956.

(20) Stober, W.; Fink, A.; Bohn, E. *J. Colloid Interface Sci.* **1968**, *26*, 62.

(21) Van Blaaderen, A.; Van Geest, J.; Vrji, A. *J. Colloid Interface Sci.* **1992**, *154*, 481.

(22) Bogush, G. H.; Tracy, M. A.; Zuckoski, C. F., IV *J. Non-Crystalline Solids* **1988**, *104*, 95.

(23) Van Helden, A. K.; Jansen, J. W.; Vrij, A. *J. Colloid Interface Sci.* **1981**, *81*, 354.

(24) Barbetta, A.; Cameron, N. R. *Macromolecules* **2004**, *37*, 320.

(25) Orioni, B.; Roversi, M.; La Mesa, C.; Asaro, F.; Pellizer, G.; D'Errico, G. *J. Phys. Chem. B* **2006**, *110*, 12129.

(26) Bonincontro, A.; Spigone, E.; Ruiz Peña, M.; Letizia, C.; La Mesa, C. *J. Colloid Interface Sci.* **2006**, *304*, 342.

(27) Wu, C.; Unterforsthuber, K.; Lilge, D.; Lüddecke, E.; Horn, D. *Part. Part. Syst. Charact.* **1994**, *11*, 145.

(28) Letizia, C.; Andreozzi, P.; Scipioni, A.; La Mesa, C.; Bonincontro, A.; Spigone, E. *J. Phys. Chem. B* **2007**, *111*, 898.

(29) Adamson, A. W. *Physical Chemistry of Surfaces*, 5th ed.; Wiley: New York, 1991; Chapter 5, p 218.

(30) Ohshima, H. *J. Colloid Interface Sci.* **2002**, *252*, 119.

(31) Vold, R. D.; Vold, M. J. *Colloid and Interface Chemistry*; Addison Wesley: Reading, MA, 1983; Chapter 6, p 212.

(32) Tang, C. J.; Neves, A. J.; Carmo, M. C. *J. Phys.: Condens. Matter* **2005**, *17*, 1687.

(33) Masci, G.; De Leonardis, P.; Mannina, L.; Capitani, D.; Diociaiuti, M.; Crescenzi, V., manuscript in preparation

(34) Dale, P. J.; Vincent, B.; Cosgrove, T.; Kijlstra, J. *Langmuir* **2005**, *21*, 12244.

(35) Dale, P. J.; Kijlstra, J.; Vincent, B. *Langmuir* **2005**, *21*, 12250.

(36) (a) Mysels, K. J. *An Introduction to Colloid Chemistry*; Interscience: New York, 1959. (b) Loeb, A. L., Overbeek, J. Th., G., Wiersma, P. H. *The Electrical Double Layer around a Spherical Colloid Particle*; MIT Press: Cambridge, MA, 1961.

(37) Heimburg, T.; Marsh, D. *Biophys. J.* **1995**, *68*, 536.

(38) Zuckermann, M. J.; Heimburg, T. *Biophys. J.* **2001**, *81*, 2458.

(39) Wind, B.; Killmann, E. *Colloid Polym. Sci.* **1998**, *276*, 903.

(40) Bevan, M. A.; Scales, P. J. *Langmuir* **2002**, *18*, 1474.

(41) Johnson, H. E. *Macromolecules* **1990**, *23*, 3367.

(42) Schneider, H. M. *Macromolecules* **1992**, *25*, 5054.

(43) Braithwaite, G. J. C. *Langmuir* **1996**, *12*, 4224.

(44) Sallustio, S.; Galantini, L.; Gente, G.; Masci, G.; La Mesa, C. *J. Phys. Chem. B* **2004**, *108*, 18876.